JOURNAL OF MATERIALS SCIENCE 33 (1998) 1857–1862

Influence of vanadium oxide on BSCCO (2 2 2 3) phase formation and related properties

A. TAMPIERI, G. CELOTTI, F. MONTEVERDE
IRTEC-CNR, via Granarolo, 64 48018 Faenza, Italy
E-mail: tampieri@irtec.bo.cnr.it

F. EL-TANTAWY, S. A. MANSOUR
Suez Canal University, Faculty of Science, Dept. of Physics, Ismailia, Egypt

The preparation of BSCCO 2 2 2 3 superconducting powder was studied with addition of V_2O_5 ranging from 0.3 to 0.5 molar index. Various compositions were prepared both containing and without Pb and subsequently treated with different firing cycles, to promote the incorporation in lattice sites of vanadium atoms. Different densification procedures were attempted and final bulk samples characterized to evaluate microstructural, mechanical and electrical properties. The addition of vanadium was found to increase the formation rate of high T_c phase and about 90% of 2 2 2 3 phase has been obtained in 80 h. However, this element was found to present an outstanding segregation trend at grain boundaries (especially with Sr) and to be responsible of a marked delay in 2 2 2 3 phase formation in respect to lead-doped samples. Transport properties seem positively affected even if considerable contamination at grain boundary and lowering in offset critical temperature are unavoidable. © *1998 Chapman & Hall*

1. Introduction

The superconducting Bi-based cuprates of the system with the general formula $Bi_2Sr_2Ca_{n-1}Cu_nO_x$ (BSCCO) are characterized by a layered complex crystalline structure, high values of the transition temperature ($T_{c,0}$) and high critical magnetic field.

The study of the influences of the various doping metals on the properties of the superconducting materials is one of the main trends aimed to improved the 2 2 2 3 phase formation rate and to increase the superconductor critical temperature above 110 K [1].

Indeed one of the most effective ways to operate in this direction seems the addition to the synthesis mixture of high valence cation oxides [2–5]. In the present study the addition of vanadium oxide because of its low melting temperature, has been attempted. It has been supposed that vanadium, even if characterized by limited solubility and low reactivity [6] in respect to BSCCO system, is very promising owing to its ability to adopt various oxidation states such as vanadium(V) and vanadium(IV) and this valence fluctuation may influence the hole-carriers' density in the copper layers through the hole reservoir effect [7]. Moreover, vanadium, because of its smaller size, compared to Bi, is susceptible to bring the Cu-layers close to each other and consequently to increase coupling effect.

2. Experimental procedure

The samples were prepared by the solid-state reaction technique, reagent grade powders of Bi_2O_3, PbO, $SrCO_3$, $CaCO_3$, CuO and V_2O_5 (purity 99.99%) were mixed in agate ball mill with the nominal compositions: Powder A = $Bi_{1.84}Pb_{.34}Sr_{1.91}Ca_{2.03}Cu_{3.06}V_xO_y$, powder B = $Bi_{1.84}Sr_{1.91}Ca_{2.03}Cu_{3.06}V_xO_y$ ($x = 0.3$, 0.35, 0.4, and 0.5) ($y \simeq 10.5$–11.3). Powders A and B were pelletized and fired in the range 700–840 °C, with intermediate grindings, for about 100 h in a box electrical furnace under static air atmosphere. Powder C was obtained starting with the same composition as powder B but fired at 880 °C for 100 h and post-annealed at 840 °C for 85 h.

BSCCO with added vanadium (0.35%) was also prepared following previous data [2] and called powder D (820 °C for 20 h, 845 °C for 40 h, 865 °C for 30 h, 830 °C for 30 h and 843 °C for 40 h, then quenched at room temperature).

The final powder A was analysed by differential thermal analysis (DTA) and thermogravimetric analysis (TGA); the measurements were performed from room temperature up to 1000 °C with heating rate of 10 °C min^{-1} in flowing air using Netzsch instrument. Powder was subsequently densified by using hot-pressing, and pressureless sintering, the latter performed on high cold uniaxially pressed (700 MPa) samples. As regards hot-pressing and pressureless sintering, the experimental conditions are reported in Table I. The powder and dense samples' morphology was analysed by scanning electron microscopy (SEM; Leica-Cambridge Ltd.) equipped with an energy dispersive X-ray (EDX) detector. Microstructural analysis was performed by X-ray diffraction techniques

TABLE I Dense samples' characteristics

Sample powder	RD (%)	F (%)	2223/2212/2201 volume fraction	T_{conset}, (K)	$T_{coeffset}$ (K)	σ (MPa)
PLS-A	87	35	84/11/5	115	86	78 ± 5
PLS-B	86	38	83/6/11	–	–	72 ± 5
PLS-C	90	42	92/5/3	110	100	74 ± 5
HP-A	97	24	64/28/8	105	50	110 ± 4

(XRD) in the 2θ range 3–51°, by means of a Rigaku diffractometer using CuK_α radiation. Sample density was measured by Archimedes' method. Mechanical characterization of dense samples was performed by Instron apparatus determining flexural strength through four-point bending strength method. Resistivity was measured by the four-point probe method, rectangular-shaped samples, cut from the sintered pellets, were provided with silver contacts. This measurement between 300 and 5 K was performed in a continuous-flow cryostat incorporated in a computer-controlled fully automatic system for temperature variation, data aquisition and processing.

The transport critical current density J_c was determined by I–V measurements carried out at 77 K and zero applied magnetic field with a voltage criterion of 1 $\mu V\,cm^{-1}$.

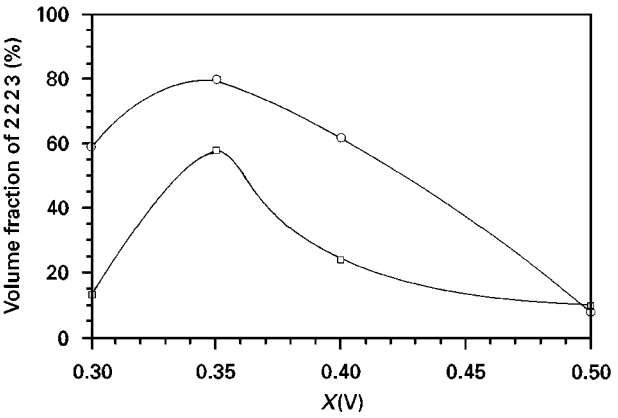

Figure 1 Volume fraction of 2223 phase obtained in function of V concentration for two different thermal treatment times. (□) 50 h; (○) 100 h.

3. Results and discussion

The amount of 2223 phase, during the formation reaction of the superconducting phase, was monitored by XRD starting from calcined powder A containing different amounts of V_2O_5. In Fig. 1 the volume fraction of 2223 into the mixture fired at 842 °C for 50 h and 100 h is reported as a function of the molar ratios of vanadium: the highest formation rate is found for the composition containing molar quantity of $V \approx 0.35$ which was used for the further investigations. It is worthwhile to mention that for $x = 0.5$, increasing firing time from 50 to 100 h, no variation in the volume fraction of 2223 phase was detected, indicating a substantial inhibition in high critical temperature phase formation.

Concerning the preparation of 2223 BSCCO powder doped with vanadium two approaches were used: the first one in which the synthesis temperature was selected immediately before the melting point of the mixture ($T \approx 842$ °C) in order to avoid partial melting phenomena accompanied by the recrystallization of 2201 phase (powder A); the second one in which the synthesis temperature reaches a maximum higher than the melting point of the mixture in order to favour the decomposition of intermediate compounds, segregating vanadium, and stimulate the dissolution and diffusion processes (powders C and D).

As regards powder A synthesis, the secondary phases accompanying the formation of 2223 phase in the various intermediate steps of the preparative process were determined by XRD and reported in Fig. 2. In the early stages mainly 2201 is observable, after 100 h about 90% of 2223 phase is obtained always accompanied by Ca_2CuO_3. The presence of very

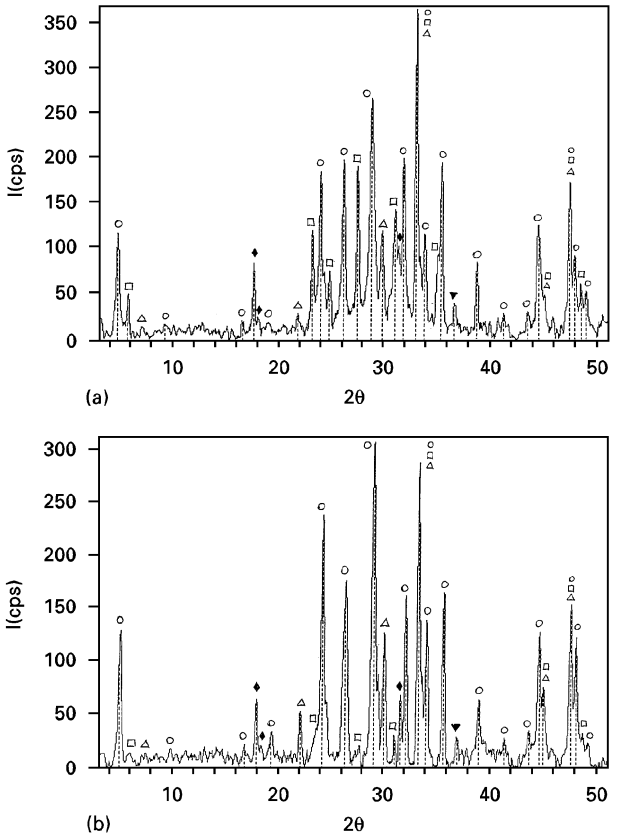

Figure 2 XRD patterns of powder A after (a) 50 and (b) 100 h of thermal treatment. (○) 2223; (□) 2212; (△) 2201; (◆) Ca_2PbO_4; (▼) Ca_2CuO_3.

stable phases, such as Ca_2CuO_3, and the absence of a reactive phase like $Bi_6(Ca,Sr)_5O_{14}$ [8] can be considered as indicators of the slackened 2223 formation in respect to the classic mixture containing lead. The

morphology of powder A in Fig. 3 is characterized by high degree of polydispersion i.e. large platelets surrounded by very small fragments; by X-ray microprobe analysis the composition of the platelets resulted in 2 2 2 3, while the rounded grains contain only Sr and V.

Although the amount of vanadium detected on average in the powder was 0.35 molar index, a detailed and statistical evaluation of the samples pointed out that vanadium segregates mainly as $Sr_3V_2O_8$ and/or $Sr_4V_2O_9$ which are stable phases even at T much higher than 850 °C and that no substitutional vanadium is included within the 2 2 2 3 phase lattice.

The high stability and melting point of the mixture $Sr_3V_2O_8$–$Sr_4V_2O_9$, verified by thermal analysis makes the role of this compound completely different from that of Ca_2PbO_4 and its segregation at grain boundary, seizing cations from the reaction site, are the causes of the low efficiency of vanadium.

Differential and thermogravimetric analysis of powder A mixture before calcination, in the temperature range 20–1000 °C, is reported in Fig. 4; chemical reactions are observable at temperature $480 \leqslant T \leqslant 940$ °C and develop via a complex process.

The T_G curve reveals a weight loss starting at $T \approx 480$ °C, i.e. lowered by about 100 °C in respect of the one detected in the mixture without vanadium. $CaCO_3$ in presence of V_2O_5 probably forms a eutectic mixing, decomposing at lower temperature. Indeed,

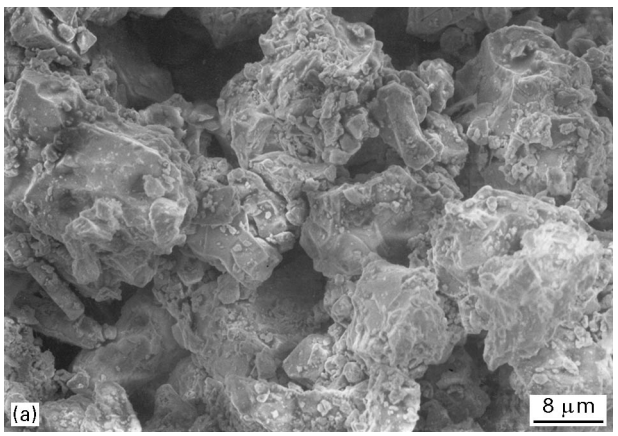

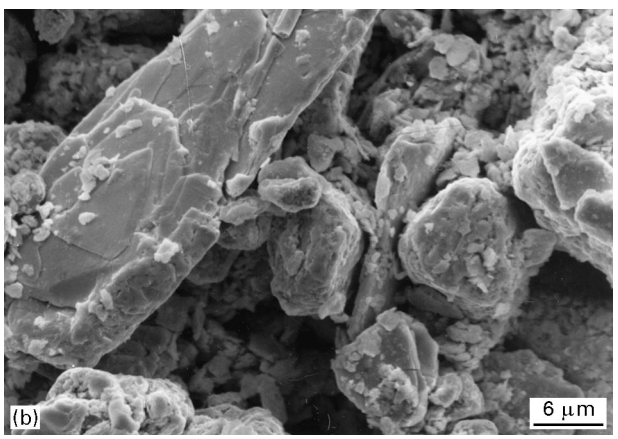

Figure 3 SEM micrographs of powders A, (a) after pre-calcination (700 °C, 3 h) and (b) after synthesis (842 °C, 100 h).

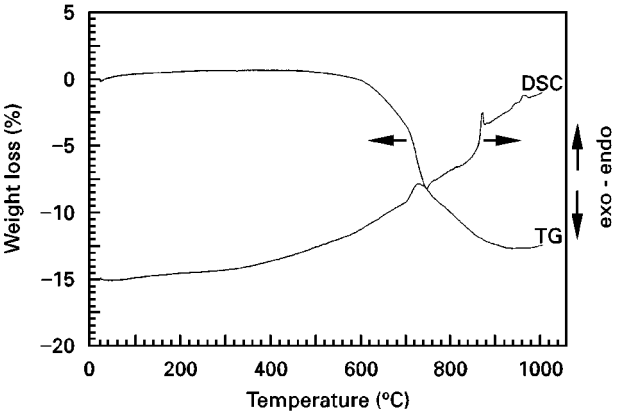

Figure 4 TG-DTA curves for powder A mixture before calcination.

a binary mixture of $CaCO_3$ and V_2O_5, in the same molar ratio as the superconducting mixture, was separately analysed showing the anticipated decomposition of $CaCO_3$; the DTA peak at 640 °C can be attributed to V_2O_5 melting and XRD pattern of the powder, obtained by thermal treatment at this temperature, shows the presence of CaO, $CaCO_3$ and $Ca_7V_4O_{17}$. As temperature increases (Fig. 4) the second step of $CaCO_3$ decomposition occurs, being completed at ~ 730 °C with a total weight loss of $\sim 9.6\%$. The second step corresponds to a weight loss of $\sim 4\%$ (some $SrCO_3$ decomposition is anticipated during the previous one of $CaCO_3$) and it is completed at about 940 °C. At low temperatures $T \approx 480$ °C the powder exhibits a multiphase composition including the original reactant phases: $SrCO_3$, $CaCO_3$ and CuO together with Ca_2PbO_4, binary oxides and 2 2 0 1 phase. To interpret the series of small peaks on DTA curve, samples of the same starting mixture were annealed for 10 min up to various temperatures and then analysed by XRD. These analyses revealed that at $T \approx 730$ °C the predominant phases are $Bi_{14}Ca_4O_{25}$ and Bi_4CaO_7. The exothermic peak at ≈ 750 °C could be attributed to the formation of $Bi_6(Ca,Sr)_5O_{14}$. For further increases of temperature up to $T \approx 800$ °C 2 2 0 1 phase appears; at $T \approx 850$ °C 2 2 1 2 phase and Ca_2PbO_4 start to form, accompanied by the contemporaneous increase of 2 2 0 1 phase. The peak with the origin at 842 °C and the top at $T \approx 865$ °C can be ascribed to the mixture incongruently melting.

In order to evaluate the single effect of vanadium and to eliminate the competitive effect of Pb powder B was prepared and analysed; in Fig. 5 XRD patterns of the different steps of the preparative procedure are reported, showing a great retard in 2 2 2 3 formation as compared to classical Pb-doped mixture. After 100 h of thermal treatment at 840 °C the 2 2 1 2 phase was still 75%.

Microprobe analysis of powder B again revealed the expected vanadium concentration but the analysis carried out at higher magnification with a probe diameter of ≈ 1 μm was not able to detect vanadium into the superconducting grains and big agglomerates with composition intermediate between $Sr_3(VO_4)_2$–$Sr_4(VO_4)_2O$ were found spread over the matrix.

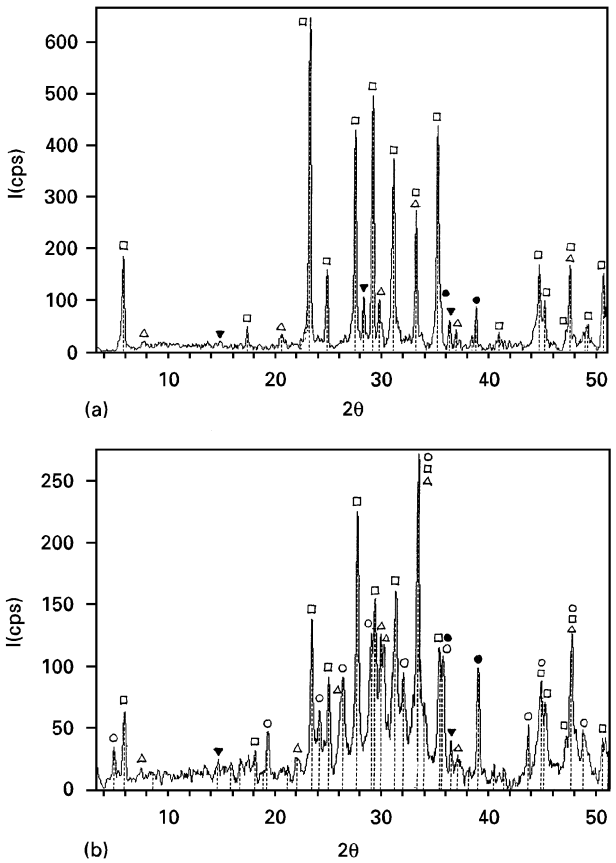

Figure 5 XRD patterns of powder B after (a) 50 and (b) 100 h of thermal treatment. (○) 2 2 2 3; (□) 2 2 1 2; (△) 2 2 0 1; (●) CuO; (▼) Ca_2CuO_3.

Generally doping with these high valency cations may lead to the lowering of the melting point of samples, but in the case of vanadium it is still 10 °C higher than the corresponding Pb-doped sample, so the results are largely lower. Even special methods used for preparing powder C and D, aimed at amplifying the melting phenomena and avoiding recrystallization of vanadium in form of the secondary phases, were not able to prevent the segregation of vanadium and strontium at the grain boundary.

After 100 h of firing at 885 °C the main products of powder C are 2 2 0 1 and Ca_2CuO_3. Subsequently powder C was annealed for 80 h at 840 °C and about 90% of 2 2 2 3 phase was attained. XRD microprobe analysis was also in this case performed statistically on BSCCO grains; however, contrarily to data previously reported in the literature, decisive evidence that vanadium has been included in the lattice of BSCCO and distinguished by contamination of segregated precipitates was not reached. Among the indirect evaluations to establish the income of vanadium into the superconducting phase structure the calculation of cell parameters has been commonly used. Because the atomic radius of vanadium is smaller than that of bismuth and if it substitutes into the BiO layers, the cell volume should decrease. The cell parameters calculated for 2 2 2 3 phase by XRD of powder C resulted in: $a = 0.5382$ and $c = 3.693$ nm that for the c axis it is very similar to that previously observed [9] for sample claimed to contain vanadium in lattice sites.

Diffractometric analysis of powder D after quenching showed the formation of 65% of 2 2 2 3, 20% of 2 2 1 2, 15% of 2 2 0 1 and Ca_2CuO_3. SEM analysis of the powder is shown in Fig. 6a, b; typical 2 2 2 3 phase platelets appear characterized by embedded polygonal dark precipitates (Fig. 6a). In Fig. 6b an intergranular area is shown full of prismatic grains. Both the described structures (precipitates and prisms) were analysed by EDS and found to be $Sr_3V_2O_8$ with small amount of $Sr_4V_2O_9$.

Using powders A, B and C different sintering processes were performed to prepare dense materials and to evaluate the effect of the specific technique on material characteristics particularly those linked to vanadium presence.

3.1. Hot-pressing

Hot pressing promotes densification attaining final density of $\approx 98\%$, even if the presence of vanadium, creating several globular agglomerates at grain boundary, acts as a disturbing agent on texturing process and final samples present low orientation factor compared to those without vanadium [10].

In the vanadium-doped samples hot pressing stimulates recrystallization of large amount of secondary phases such as 2 2 1 2 and 2 2 0 1 at the triple point and around the grain surface. The resistivity curve in Fig. 7 shows an onset temperature at $T = 110$ K but an offset temperature $T = 50$ K. This proves that intergranular properties are extremely degraded and that superconducting grain critical temperature is not influenced by vanadium. The effect of vanadium stimulating densification and reinforcing grain boundary region, involves high values of σ but also the recrystallization of large amounts of non-superconducting phases acting as a barrier for current circulation.

3.2. Pressureless sintering

All the above mentioned phenomena are less stressed in pressureless sintered samples [11]; in fact this process reduces the re-crystallization phenomena, density and the homogeneity of grain boundary region distribution. As a consequence more localized impurities have a minor influence on the offset value of the critical temperature that increases at $T = 86$ K. Obviously, the resulting mechanical properties of these samples are poorer, see Table I. Actual microstructural defects, mainly located at the grain boundary, contribute to create an alternative route to the insulating region existing as junction among grains; the result is a minor influence of the non-superconducting phase (even if present in large amounts) on the current circulation path (Fig. 7). In Fig. 8a the fracture surface of sample PLS-B is reported showing the peculiar morphology of particles segregated into the superconducting matrix. In Fig. 8b the points in which EDS analysis was performed are marked: A identifies those segregations whose composition is intermediate between $Sr_3V_2O_8$ and $Sr_4V_2O_9$. B, D and E correspond to platelets of 2 2 2 3 phase, while point C composition results a mixture of (Ca, Sr)CuO_2 and Bi_2CuO_4.

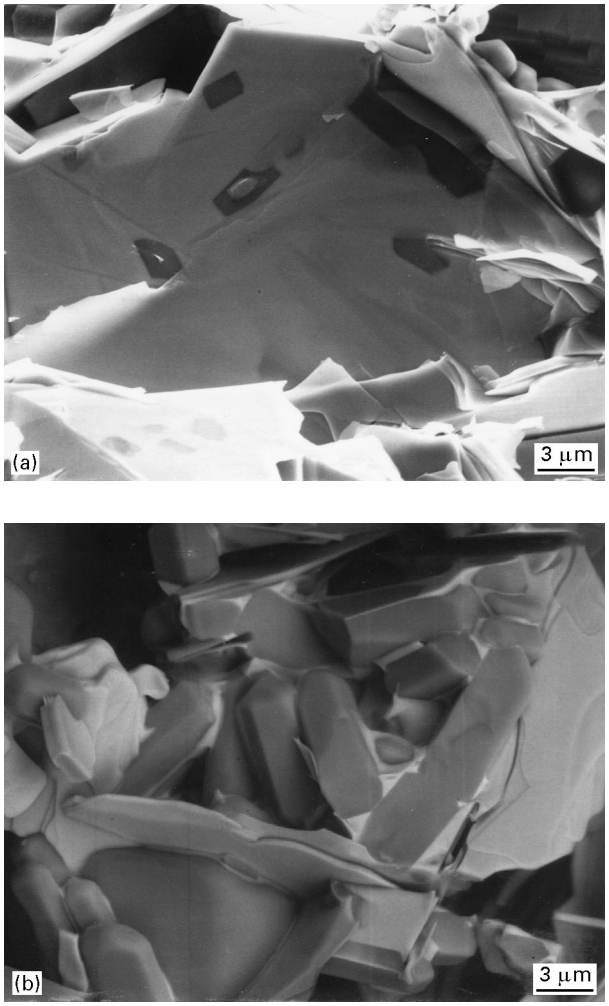

Figure 6 SEM micrographs of powder D agglomerates showing different Sr–V–O precipitate morphology: (a) within matrix platelets, (b) isolated prisms.

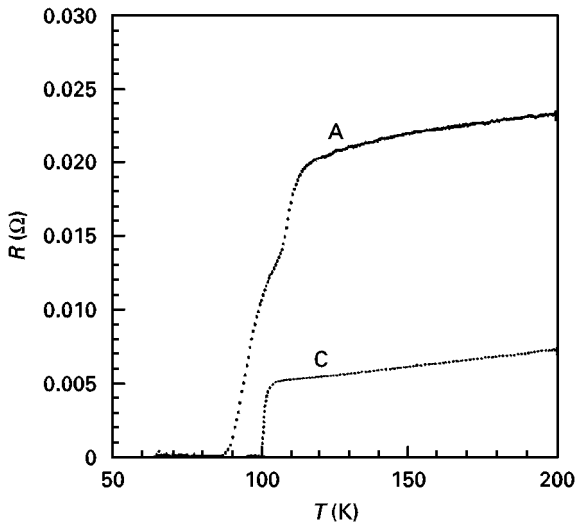

Figure 7 Resistivity versus temperature curves for PLS-A and PLS-C samples.

The same densification procedure was also performed using powder C: morphological evaluation reveals in this case a lot of agglomerates rich in vanadium, even if the presence of big segregations containing V and Sr seems reduced and substituted by

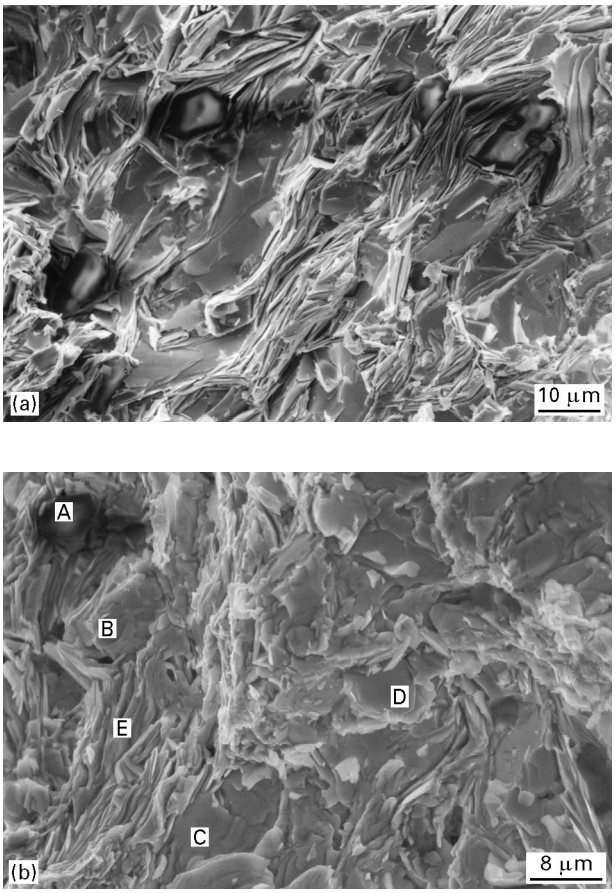

Figure 8 SEM micrographs showing general morphology of fracture surface of sample PLS-B (a) and detail with microprobe analysis points marked (b).

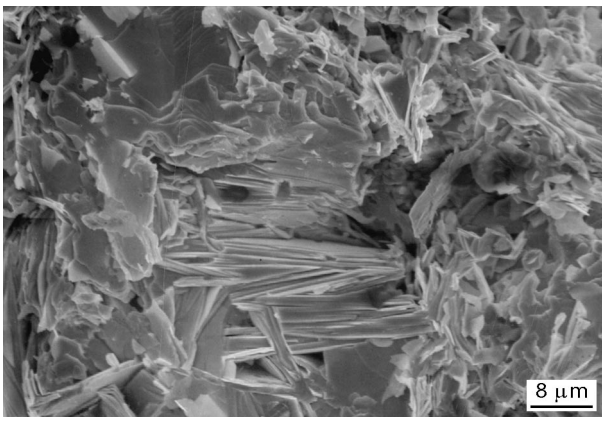

Figure 9 SEM micrograph showing fracture surface of sample PLS-C.

smaller grains more uniformly distributed. In Fig. 9 morphology of fracture surface of PLS-C is reported showing misoriented islands of well-aligned grains.

The critical temperature became 100 K because of the straight fall and the absence of a tail in the resistivity curve, largely justified by the higher amount of 2223 phase, orientation factor and connectivity among grains. Indeed, the reduction in the dimension of segregated precipitates and the modification in their distribution as shown in Fig. 9 can explain the formation of improved links among grains.

Critical current density of PLS-C sample, measured at 77 K, was found to be $J_c = 200\ A\,cm^{-2}$. To justify such a relatively high value for a bulk sample previous authors put forward the hypothesis that vanadium causes planar defects along the *ab* plane, which have been considered effective in generating flux pinning centres [9].

4. Conclusions

BSCCO powders doped with vanadium were prepared with different procedures and composites: powder A presents large segregations of $Sr_3V_2O_8$ and $Sr_4V_2O_9$ and vanadium cannot be detected into 2223 grains by microprobe analysis. The kinetics of 2223 phase formation were improved with respect to undoped samples while they were slackened if compared with lead-doped ones.

Indeed, a comparison between powder A and B shows that the presence of Pb implies a selective substitution of Bi (pointed out by microprobe analysis) while vanadium, forming secondary phases at the grain boundary, subtracts Sr from the reaction site.

By thermal analysis the formation process and the reaction intermediates involved in the V-doped BSCCO 2223 synthesis were elucidated.

Using three different powders, dense samples were prepared by various sintering techniques. Hot-pressed samples presented high density but a considerable degradation in critical temperature because of diffuse recrystallization phenomena.

Pressureless sintered samples prepared with powder synthesized at high temperature (powder C) reached a density around 90% and, despite the limited orientation degree, is characterized by J_c and T_{c_0} values typical of the 2223 superconductor.

Generally we can conclude that doping with V leads to a delay in 2223 phase formation respect to Pb-doped sample; only high temperature treatment seems to promote the complete formation of 2223 phase.

Dense samples prepared by V-doped powders were characterized by final density and mechanical properties not significantly different from undoped ones; on the contrary the amount of 2223 phase in doped samples is noticeably reduced by large recrystallization of 2212 and 2201 phase, which results in a lowering of orientation degree and T_{c_0} value, particularly for hot-pressed samples. Only pressureless sintered samples prepared with powder C show electrical properties unaffected by vanadium doping.

In summary, and in contrast with previous data, all the performed experiments demonstrated the almost complete segregation of vanadium combined with strontium and its reluctance to enter the BSCCO lattice.

References

1. S. A. SUNSHINE and T. SIEGRIST, *Phys. Rev. B* **38** (1988) 893.
2. X. YING, Z. Z. SHENG, F. T. CHAN, P. C. FUNG and K. W. WONG, *Solid State Commun.* **76** (1990) 1347.
3. *Idem., ibid.* **76** (1990) 1351.
4. Y. R. LI and B. C. YANG, *J. Mater. Sci. Lett.* **13** (1994) 594.
5. M. E. YAKINCI, I. AKSOY and M. CEYLAN, *J. Mater. Sci.* **31** (1996) 2865.
6. T. KANAI, T. KAMO and S. MATSUDA, *Jpn. J. Appl. Phys.* **28** (1989) L551.
7. P. C. W. FUNG, Z. C. LIN, Z. M. LIU, X. YING, Z. Z. SHENG, F. T. CHAN, K. W. WONG, X. YONG-NIAN and W. Y. CHING, *Solid State Commun.* **75** (1990) 211.
8. A. TAMPIERI, E. LANDI and G. CELOTTI, *Physica C* **254** (1995) 342.
9. P. C. W. FUNG, J. C. L. CHOW and Z. L. DU, *Supercond. Sci. Technol.* **7** (1994) 397.
10. G. CELOTTI, A. TAMPIERI, R. MASINI and M. C. MALPEZZI, *Physica C* **225** (1994) 346.
11. G. CELOTTI, A. TAMPIERI, E. LANDI and R. MASINI, *IV EuroCeramics* **6** (1995) 219.

Received 24 October 1996
and accepted 17 December 1997